scientific reports

Check for updates

OPEN

Dusp1 in osteolytic diseases-mechanisms and therapeutic potential

Boyu Liu[1,2,5], Ming Lei[1,5], Baicheng Wan[1], Yanbing Feng[1], Yilin Teng[1], Deshuang Xi[1], Shou Chen[1,2], Gaofeng Zeng[3]✉ & Shaohui Zong[1,4]✉

Osteolytic diseases are a significant and escalating global public health issue, driven by the acceleration of population aging and the rising incidence of degenerative, metabolic, and neoplastic diseases. The primary therapeutic strategy for osteolytic diseases is to suppress the bone resorption activity of osteoclasts. Dusp1 is a member of the serine/threonine inducible nuclear phosphatase family and has significant anti-inflammatory effects. In this study, Dusp1 overexpression was induced via lentiviral transfection. We found that Dusp1 antagonized RANKL stimulation, mediated the MAPK signaling pathway, and downregulated the key downstream transcription factors c-FOS and NFATc1, thereby reducing the expression of osteoclast-specific genes. Furthermore, Dusp1 reduced the number and activity of osteoclasts both in vivo and in vitro, leading to a diminished bone resorption function. In addition, the results of animal experiments demonstrated that Dusp1 protected mice from LPS-induced skull osteolysis. Overall, our study reveals that Dusp1 suppresses osteoclast formation and activity by downregulating the MAPK/c-FOS/NFATc1 signaling pathway. These findings suggest the potential of Dusp1 to protect against osteolytic diseases.

Keywords Dusp1, Overexpression, Lentivirus, Osteoclast, Osteolysis, MAPK

Bone serves as a crucial locomotive organ, continuously undergoing remodeling to maintain its supportive and protective roles for the body. A balanced bone homeostasis between formation and resorption is a prerequisite for constant bone remodeling[1]. As the sole executor of bone resorption, osteoclast is essential for the maintenance of bone homeostasis. However, excessive osteoclast activity can disrupt bone homeostasis and lead to pathological osteolysis. And pathological osteolysis contributes to many bone or joint disorders, including osteoporosis, arthritis, periodontitis, gout, and tumor-induced osteolysis[2].

Osteoclasts belong to the monocytic/macrophage lineage and originate from hematopoietic stem cells[3]. The differentiation and maturation of osteoclasts are primarily driven by two key cytokines: macrophage-colony stimulating factor (M-CSF) and receptor activator of NF-κB ligand (RANKL)[4] Osteoclast precursor cells proliferate in response to M-CSF and differentiate into mature osteoclasts upon exposure to RANKL[5,6]. Upon binding of RANKL to its receptor on osteoclast precursors, the intracellular signaling molecule tumor necrosis factor (TNF) receptor-associated factor 6 (TRAF6) is activated, which in turn triggers several downstream signaling pathways, including mitogen-activated protein kinase (MAPK) and nuclear factor-kappa B (NF-κB)[7]. This activation leads to the expression of key transcription factors such as cellular proto-oncogene Fos (c-FOS) and nuclear factor of activated T cell cytoplasmic 1 (NFATc1). NFATc1 then enters the nucleus and triggers the expression of osteoclast-specific genes, including cathepsin K (CTSK), matrix metallopeptidase 9 (MMP9), acid phosphatase 5 (ACP5) and the d2 subunit of the V-ATPase proton pump (ATP6V0d2), which work together to further promote the formation of mature osteoclasts with bone resorption function[8].

Various classes of anti-resorptive drugs are currently employed to treat osteolytic conditions, but each comes with its own set of drawbacks[9]. For instance, patients who use bisphosphonates may discontinue treatment because of significant gastrointestinal discomfort and musculoskeletal pain[10]. Prolonged use of bisphosphonates has also been associated with severe complications such as osteonecrosis of the jaw and atypical

[1]Department of Spine Osteopathia, The First Affiliated Hospital of Guangxi Medical University, Guangxi Medical University, No. 6, Shuangyong Road, Nanning 530021, Guangxi, China. [2]Department of Orthopedics, Liuzhou Worker's Hospital, The Fourth Affiliated Hospital of Guangxi Medical University, Liuzhou 545000, Guangxi, China. [3]Department of Nutrition and Food Hygiene, College of Public Hygiene of Guangxi Medical University, No. 22, Shuangyong Road, Nanning 530021, Guangxi, China. [4]Wuming Hospital of Guangxi Medical University, Guangxi Medical University, Nanning 530021, Guangxi, China. [5]Boyu Liu and Ming Lei contributed equally to this work. ✉email: zenggaofeng@gxmu.edu.cn; zongshaohui@gxmu.edu.cn

femoral fractures[11]. Estrogen and selective estrogen receptor modulators are typically recommended only for postmenopausal women under 60 due to risks including breast cancer, gallbladder disease, stroke, and deep vein thrombosis[12]. Romosozumab, the only agent that simultaneously promotes osteogenesis and inhibits osteolysis, faces limitations in its use due to the high cost and cardiovascular risks[13]. Besides, interruption of any drug for any reason may lead to serious consequences, including acute bone mass loss or fragility fracture[14]. Therefore, combinational and sequential therapies are new response strategies for the treatment of these diseases[15]. In this context, it is particularly important to develop novel therapeutic approaches targeting osteoclast bone absorption.

Dual specificity phosphatase 1 (Dusp1), also known as MAP kinase phosphatase 1 (Mkp1), belongs to the serine/threonine inducible nuclear phosphatase family[16]. By removing phosphate groups from phosphorylated serine/threonine residues, Dusp1 inactivates MAPKs and regulates inflammation and immunity. Previous studies have demonstrated that Dusp1 reduces intracellular inflammation by inhibiting the MAPK signaling pathway[17]. Coincidentally, MAPK signaling pathway is also one of the key pathways regulating osteoclastogenesis[18]. This makes us wonder, what role does Dusp1 play in osteoclasts and osteolytic diseases? In fact, there are indeed some associations between Dusp1 and bone homeostasis. Gene analysis in humans and mice reveals significantly lower Dusp1 expression in older individuals compared to younger ones[19,20]. More interestingly, lower Dusp1 expression in mice caused more inflammatory bone loss[21]. These findings highlight the immense potential of Dusp1 in the treatment of osteolytic diseases. Therefore, we investigated the role and molecular mechanism of Dusp1 in osteoclast formation and osteolysis by overexpression lentivirus transfection.

Results

Lentivirus transfection effectively regulated Dusp1 expression in osteoclasts

To assess the efficiency of lentiviral transfection, green fluorescent protein (GFP) imaging was performed. Images were acquired 72 h after BMMs were transfected with NC or Dusp1 overexpression lentivirus. The images showed that more than 95% of the cells were successfully transfected (Fig. 1A). Further analysis using qPCR demonstrated that the relative expression of Dusp1 mRNA in the LV-Dusp1 group was 30.1 times higher than in the Blank group during osteoclast differentiation (Fig. 1B). This increase was corroborated by western blot results, which confirmed that Dusp1 protein levels were markedly elevated via overexpression lentivirus transfection (Fig. 1C, D). These findings indicate that lentiviral transfection was highly effective, significantly upregulating both Dusp1 mRNA and protein expression in osteoclasts.

Dusp1 overexpression suppressed RANKL-induced osteoclast differentiation and activity in vitro

To explore whether Dusp1 interferes with RANKL-induced osteoclast differentiation, BMMs were cultured with osteoclastogenic medium for 6 days. F-actin ring staining results showed that Dusp1 overexpression via lentivirus transfection significantly suppressed the number and area of F-actin rings (Fig. 2A–C). Additionally, TRAcP staining revealed visible fewer mature osteoclasts in LV-Dusp1 group compared to LV-NC and Blank groups (Fig. 3A, B). A further experiment was performed to examine the bone resorption capacity of osteoclasts. Analysis of electron microscope images found that the bone resorption area of LV-Dusp1 group was significantly smaller than that of LV-NC group and Blank group (Fig. 3C, D). Taken together, Dusp1 suppressed RANKL-induced osteoclast differentiation and activity in vitro.

Dusp1 overexpression downregulated osteoclast-specific genes expression

To explore how Dusp1 regulates the expression of osteoclast-specific genes during osteoclast differentiation, qPCR was used to quantify the mRNA levels of Ctsk, Fos, Nfatc1, Mmp9, Acp5, and Atp6v0d2. As can be seen from Fig. 4A–F, the levels of these mRNAs were significantly improved by RANKL stimulation. However, treatment with Dusp1 overexpression lentivirus transfection attenuated this RANKL stimulating and downregulated the mRNA levels. Besides, western blot analysis confirmed that Dusp1 overexpression lentivirus transfection significantly decreased the protein expression of CTSK (at 3 and 5 days after RANKL stimulation), NFATc1 and c-Fos (at 1, 3 and 5 days after RANKL stimulation) (Fig. 4G–J). It follows that Dusp1 restrains osteoclast differentiation and activity via downregulating osteoclast-specific genes.

Dusp1 overexpression inhibited MAPK signaling in osteoclasts

Given that protein synthesis of NFATc1, c-Fos and CTSK is modulated by the upstream MAPK signaling pathway, we examined the levels of MAPK member proteins at the beginning of osteoclast differentiation. We found that RANKL stimulation led to the immediate phosphorylation and activation of JNK, ERK, and P38. However, treatment with Dusp1 overexpression lentivirus transfection significantly inhibited p-JNK, p-ERK and p-P38 at 5–20 min post-RANKL stimulation (Fig. 5A–D). These findings uncovered that Dusp1 can inhibit MAPK signaling, which is likely a potentially important molecular mechanism for suppressing osteoclast differentiation.

Dusp1 overexpression prevented LPS-induced mice skull osteolysis

Finally, we assessed the protective capacity of Dusp1 in vivo. An animal model of LPS-induced mice skull osteolysis was constructed. Significant bone resorption resulting from LPS injection was observed on the reconstructed 3D images of micro-CT. In contrast, the LPS + LV-Dusp1 group exhibited substantially smaller bone resorption area on the mice skulls (Fig. 6A). Further analysis of bone parameters suggested that the bone volume/tissue volume ratio, number of porosity, and percentage of porosity were significantly lower in the LPS + LV-Dusp1 group compared with the LPS group and LPS + LV-NC group (Fig. 6B–D). Moreover, histological analysis via H&E staining indicated better bone integrity in the LPS + LV-Dusp1 group (Fig. 7A). Meanwhile, quantification of TRAcP staining showed a lower number of TRAcP-positive osteoclasts and a smaller area of TRAcP-positive

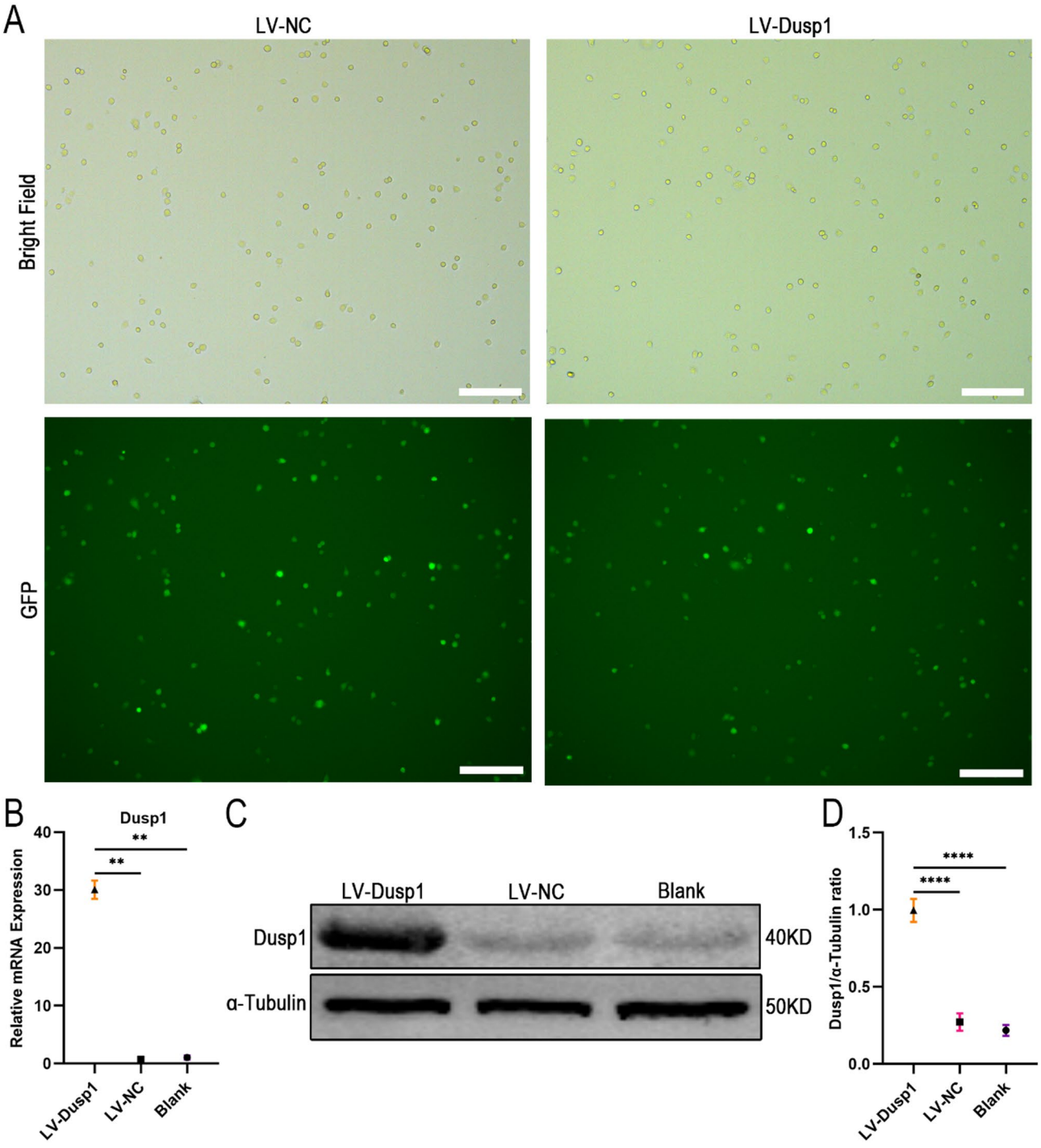

Fig. 1. Lentivirus transfection regulated Dusp1 overexpression in osteoclasts. (**A**) Representative GFP images of osteoclasts transfected with NC or Dusp1 overexpression lentivirus. (**B**) Quantification of Dusp1 mRNA expression in osteoclasts overexpressing Dusp1 or not, using qPCR. (**C**) Representative western blot images of Dusp1 in osteoclasts overexpressing Dusp1 or not. To enhance clarity and conciseness, gels and blots were cropped. The original, uncropped images are provided in Supplementary Figure S3. The samples of each group were divided from the same experiment and were processed in parallel. (**D**) Quantification of Dusp1 protein expression by gray value analysis relative to α-Tubulin. Data are presented as mean ± SD (n = 3). $^{**}p < 0.01$, $^{****}p < 0.0001$.

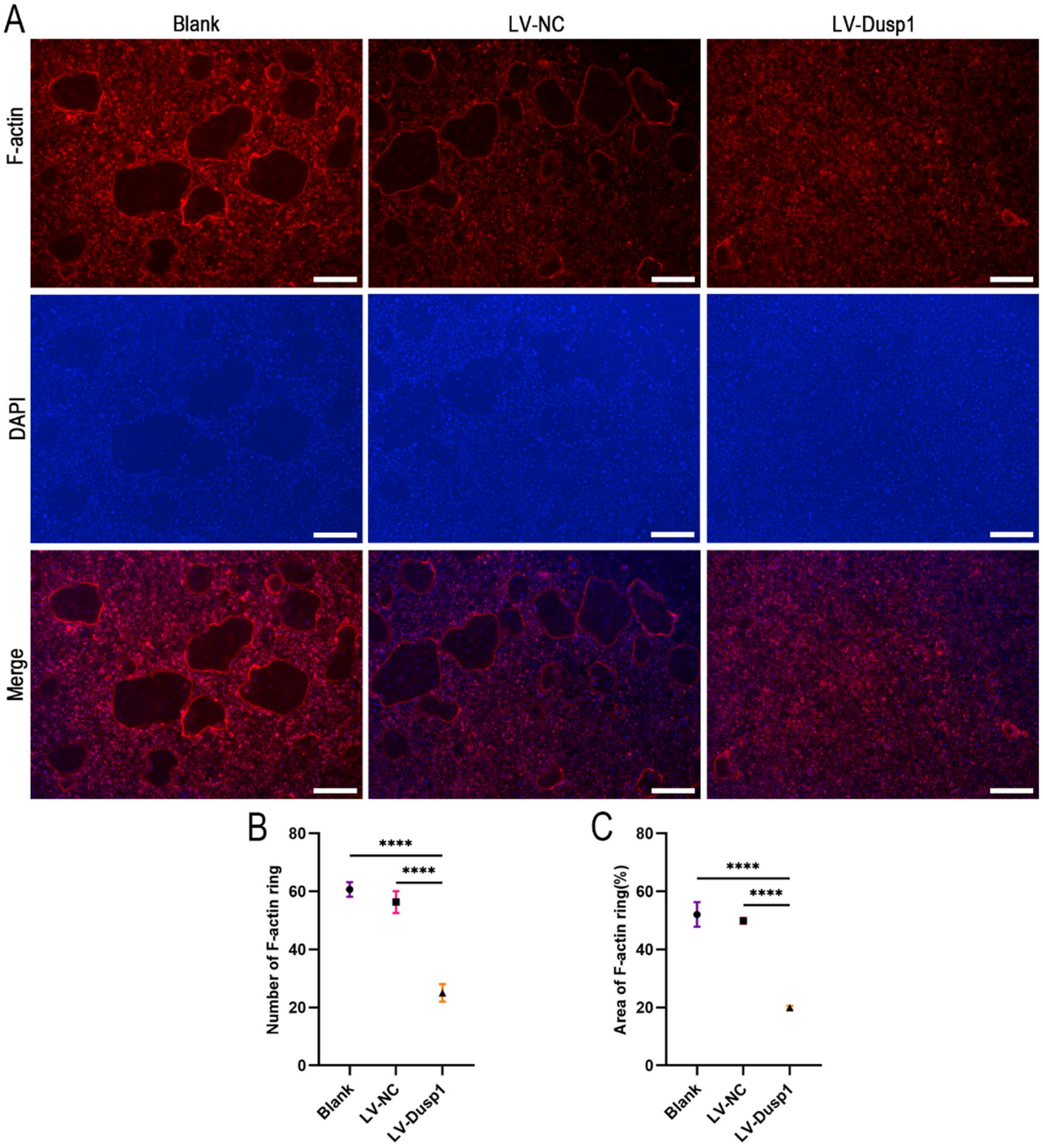

Fig. 2. Dusp1 overexpression reduced the number and area of F-actin ring in osteoclasts. (A) Representative images of F-acting ring staining (scale bar = 500 μm). (B, C) Quantification of the number of F-actin ring and the area of the F-actin ring. Data are presented as mean ± SD (n = 3). $^{****}p < 0.0001$.

osteoclasts per bone surface (Oc.S/BS) in the LPS + LV-Dusp1 group (Fig. 7B, C). It was evident from these results that Dusp1 overexpression reduced osteoclast number and activity in vivo, thereby preventing LPS-induced osteolysis.

Discussion

Bone homeostasis of formation and resorption sustains bone health. Excessive enhancement of bone resorption disrupts bone homeostasis and causes pathologic osteolytic diseases[22]. Therefore, the main therapeutic target of osteolytic diseases is to suppress osteoclast differentiation and activity. While various drugs are available to attenuate osteoclast-mediated bone resorption through different mechanisms, they often come with significant

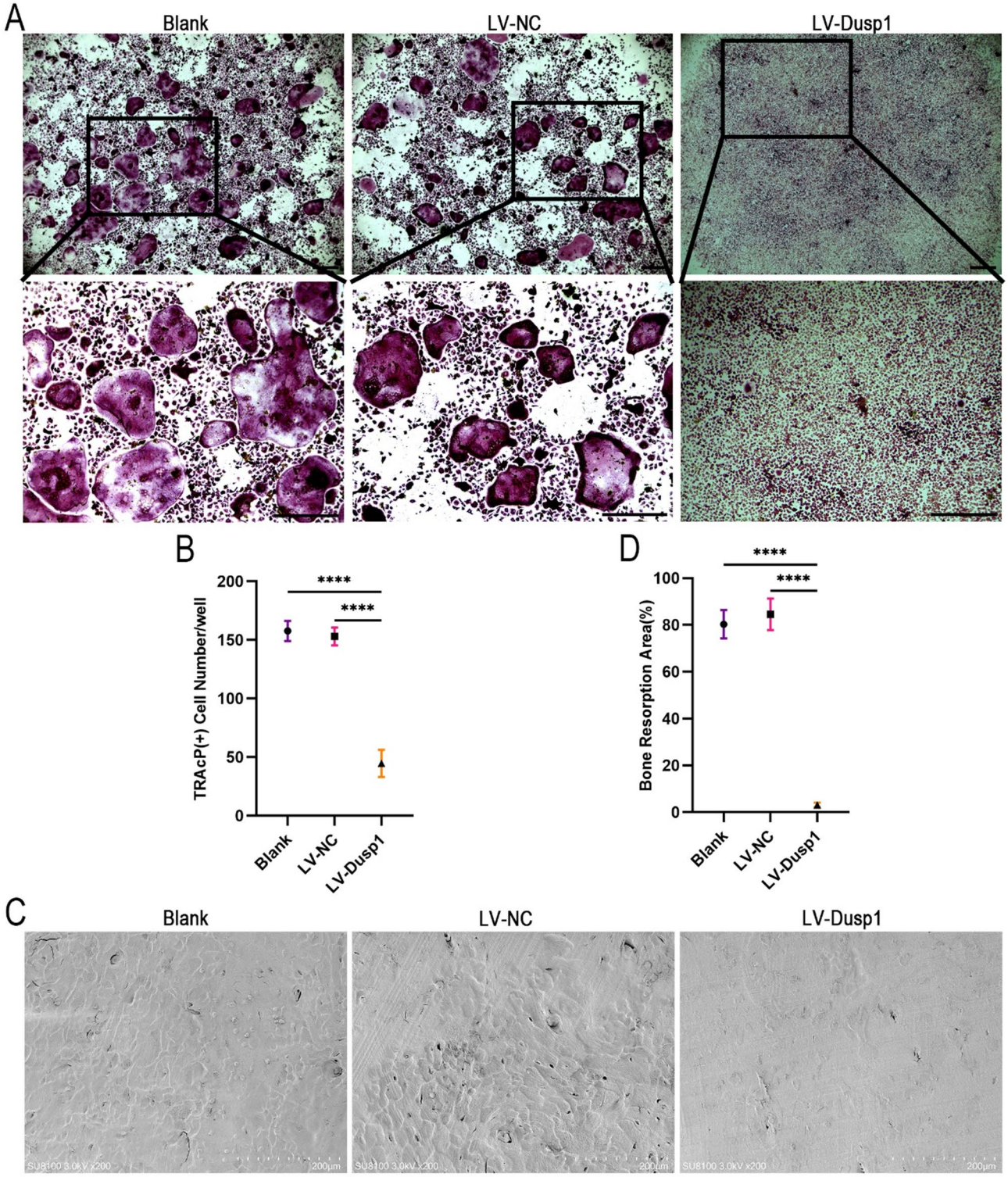

Fig. 3. Dusp1 overexpression suppressed differentiation and bone resorption capacity of osteoclasts in vitro. (**A**) Representative images of TRAcP staining (scale bar = 500 μm). (**B**) Quantification of the number of TRAcP-positive osteoclasts (nuclei ≥ 3) in each well. (**C**) Representative electron microscope scanning images of bone slices (scale bar = 200 μm). (**D**) Quantification of the bone resorption area. Data are presented as mean ± SD (n = 3). ****$p < 0.0001$.

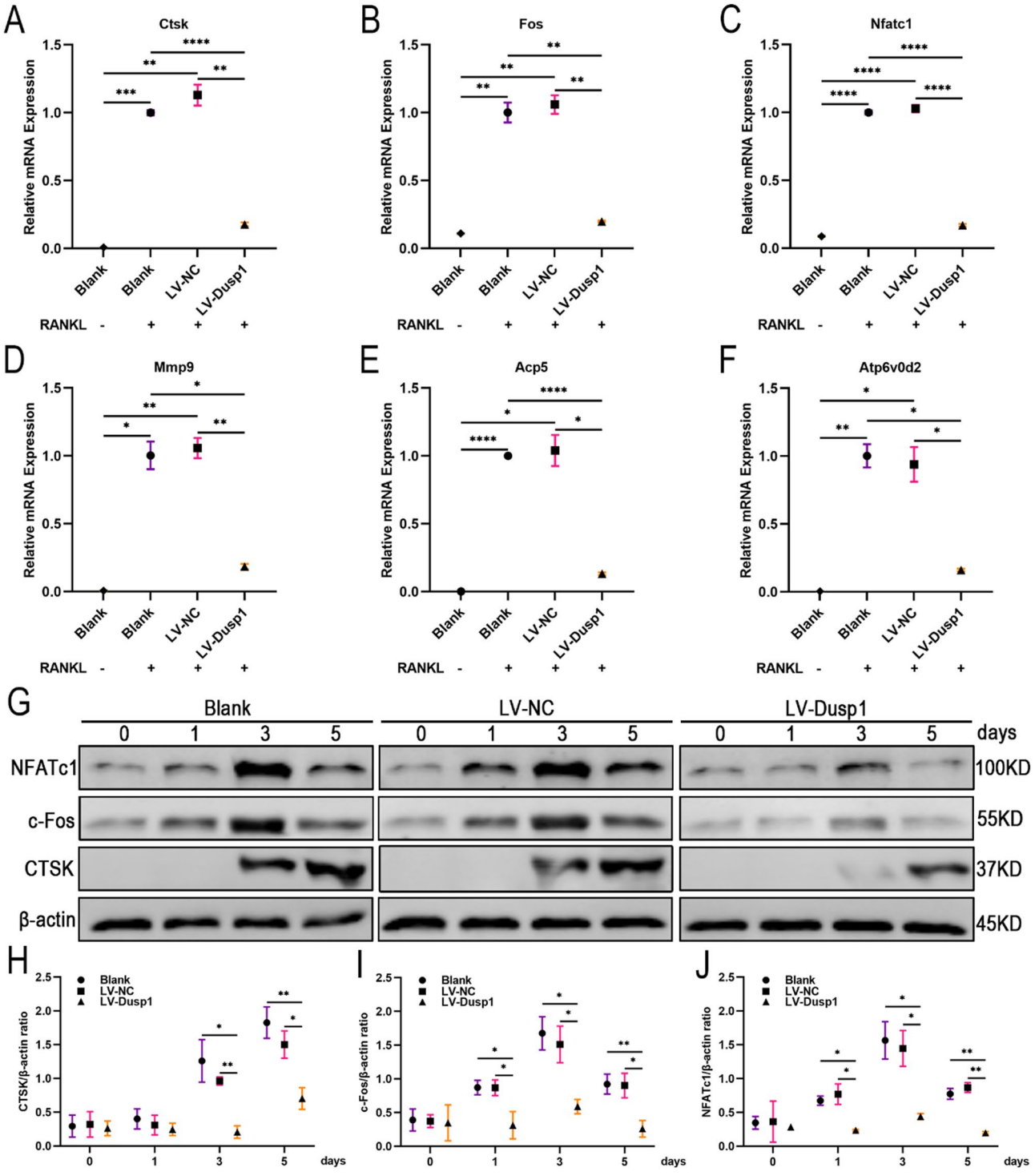

Fig. 4. Dusp1 overexpression modulated mRNA and protein expression in osteoclasts. (A-F) qPCR analysis of mRNA levels for Ctsk, Fos, Nfatc1, Mmp9, Acp5, and Atp6v0d2 in osteoclasts overexpressing Dusp1 or not. (G) Representative western blot images of NFATc1, c-Fos, and CTSK in osteoclasts overexpressing Dusp1 or not. To enhance clarity and conciseness, gels and blots were cropped. The original, uncropped images are provided in Supplementary Figure S8. The samples of each group were divided from the same experiment and were processed in parallel. (H-J) Quantification of NFATc1, c-Fos, and CTSK protein expression by gray value analysis relative to β-actin. Data are presented as mean ± SD (n = 3). *$p < 0.05$, **$p < 0.01$, ***$p < 0.001$, ****$p < 0.0001$.

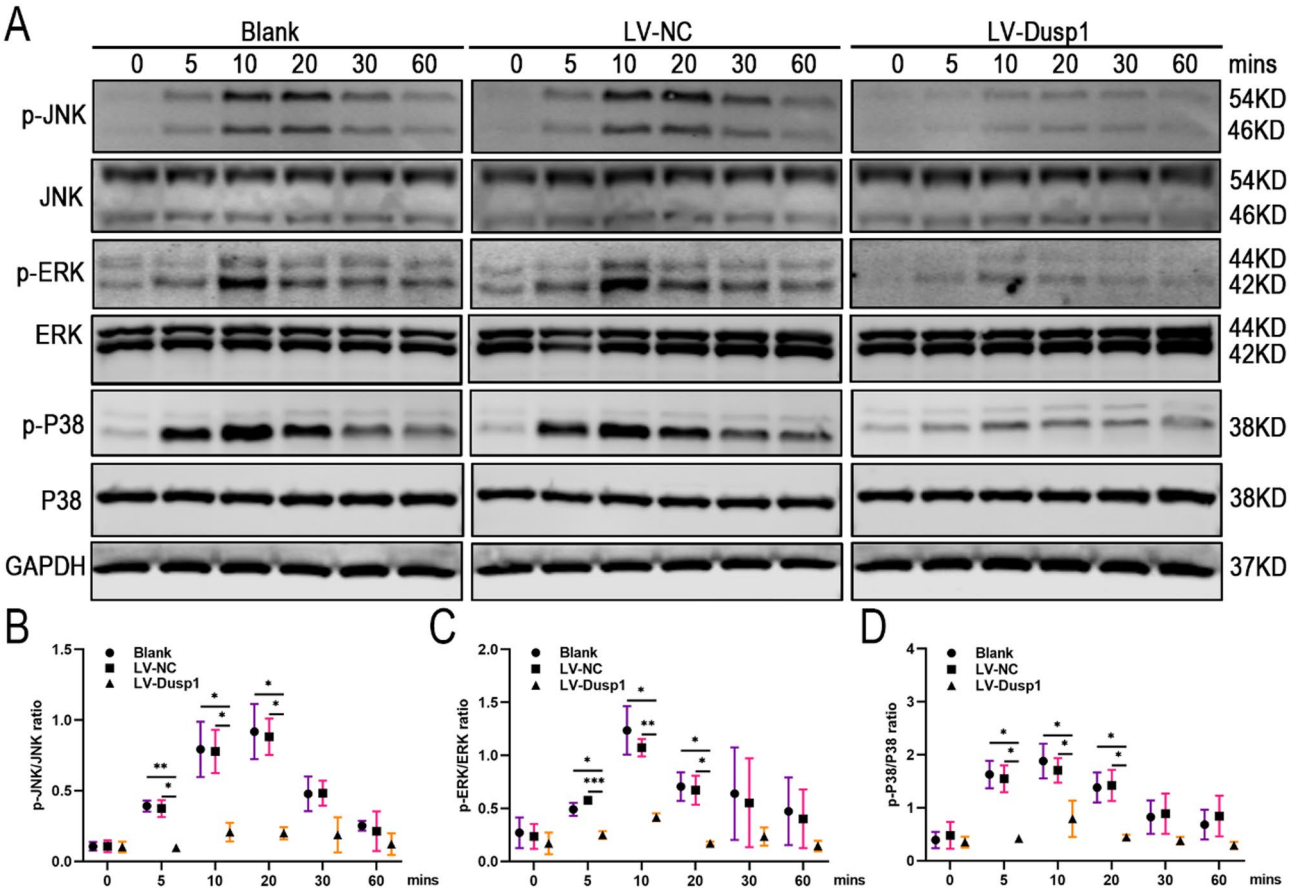

Fig. 5. Dusp1 overexpression inhibited the RANKL-induced MAPK signaling pathway in osteoclasts. (A) Representative western blot images of MAPK signaling pathway proteins (p-JNK, JNK, p-ERK, ERK, p-P38, P38) in osteoclasts overexpressing Dusp1 or not. To enhance clarity and conciseness, gels and blots were cropped. The original, uncropped images are provided in Supplementary Figure S9 and 10. The samples of each group were divided from the same experiment and were processed in parallel. (B-D) Quantification of the phosphorylated proteins p-JNK, p-ERK, and p-P38, normalized to their corresponding total protein levels. Data are presented as mean ± SD (n = 3). $^{*}p < 0.05$, $^{**}p < 0.01$, $^{***}p < 0.001$.

side effects[23]. Serious adverse events may lead to a sudden interruption of treatment, which results in great harm to patients. As a result, combinational and sequential therapies have become more common, highlighting the urgent need to develop novel therapeutic approaches for osteoclast inhibition. Given its known roles in anti-inflammatory processes and bone mass maintenance in other conditions[24], Dusp1 is a potential target in the therapy of osteolytic diseases. This study demonstrates that Dusp1 inhibits osteoclast differentiation and bone resorption activity by negatively regulating the MAPK signaling pathway in vivo. Moreover, Dusp1 mitigated LPS-induced osteolysis in vivo.

Lentiviral transfection, as a gene therapy approach, can regulate target gene expression in host cells. However, the efficiency of lentiviral transfection is influenced by multiple factors, including viral titer, multiplicity of infection, host cell compatibility, and cellular state[25]. Even if lentiviral transfection is successful, viral genome integration failure or unstable target gene expression may still occur. The innate immune response or epigenetic mechanisms of the host cell may prevent the success of gene therapy[26]. In this study, lentiviral transfection exhibited high efficiency in osteoclasts. Furthermore, lentiviral overexpression treatment significantly upregulated Dusp1 expression in osteoclasts. The actin cytoskeleton provides structural support for osteoclast morphology and is essential for bone resorption. The sealing ring formed by actin fibers isolates the bone resorption area from the surrounding environment, preventing acid and enzyme leakage[27]. Actin fibers also form a highly folded and branched structure known as the ruffled border. The ruffled border enhances osteoclast-bone surface interaction and facilitates the precise release of acids and enzymes[28]. Our experiments demonstrate the impact of Dusp1 on osteoclasts in vitro. F-actin and TRAP staining revealed that Dusp1 suppresses osteoclast differentiation. Specifically, Dusp1 significantly decreased the number of both mature osteoclasts and associated F-actin rings. Furthermore, bone resorption assay indicated that Dusp1 attenuated the bone resorption function of osteoclasts. Therefore, we further explored the molecular mechanism by which Dusp1 acts on osteoclasts.

Responding to the extracellular RANKL stimulation, osteoclast precursor cells gradually differentiate into mature osteoclasts[29]. NFATc1 is a crucial transcription factor during osteoclast differentiation and activation. Multiple intracellular signaling pathways activated by RANKL stimulation initiate NFATc1 synthesis[30].

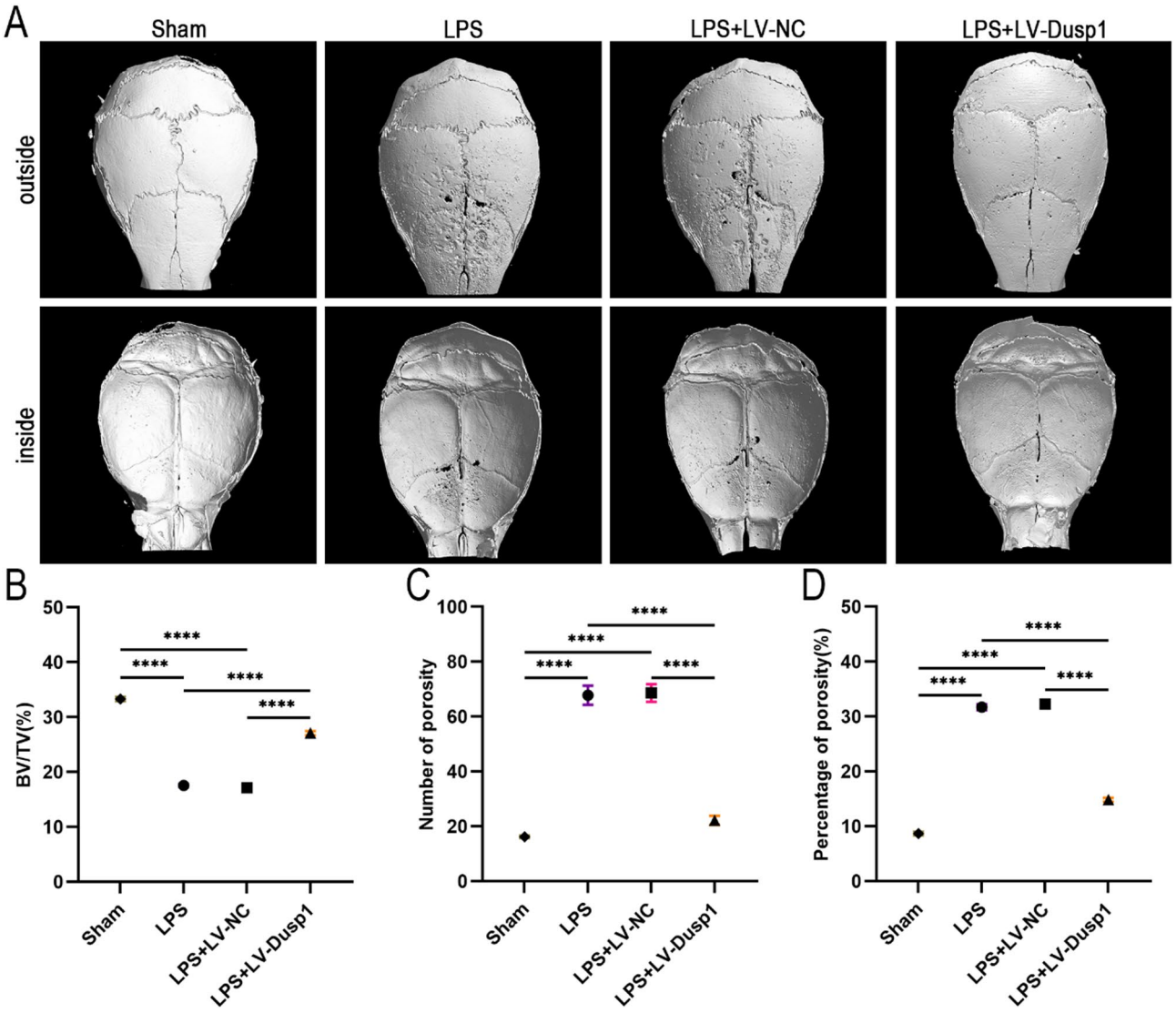

Fig. 6. Dusp1 overexpression prevented LPS-induced mice skull osteolysis. (**A**) Representative micro-CT images of the mice skulls in each group. (**B**–**D**) Quantification of bone volume/tissue volume ratio (BV/TV), number of porosity, and percentage of porosity. Data are presented as mean ± SD (n = 5). $^{****}p < 0.0001$.

Additionally, NFATc1 combines with its own promoter to complete automatic amplification[31]. Once transported into the nucleus, NFATc1 induces the expression of CTSK, Mmp9, Acp5 and Atp6v0d2[32]. These osteoclast-specific genes further promote osteoclast fusion and maturation. More importantly, they facilitate the release of acid to dissolve inorganic mineral and digestive enzymes to digest organic matrix. At this stage, osteoclasts perform the function of bone resorption[33]. C-Fos is another necessary transcription factor that regulates osteoclasts. By heterodimerizing with the proto-oncogene c-Jun, c-Fos form the activator protein 1 (AP-1) complex[34]. The AP-1 complex greatly promotes the downstream induction and automatic amplification of NFATc1[35]. Moreover, the AP-1 complex also enters the nucleus and cooperates with NFATc1 to induce osteoclast-specific genes[36]. Through qPCR and western blot analysis, we found that Dusp1 overexpression via lentiviral transfection treatment reduced the protein expression of NFATc1, c-Fos and CTSK, as well as the mRNA expression of Ctsk, Fos, Nfatc1, Mmp9, Acp5 and Atp6v0d2. These findings were consistent with the effect of Dusp1 on suppressing osteoclast differentiation and activity. These results suggest that Dusp1 down-regulates the osteoclast transcription factors c-FOS and NFATc1 to inhibit osteoclast-specific genes, thereby interfering with osteoclast differentiation and activity.

MAPK signaling pathways play a crucial role in regulating inflammation and immunity by translating extracellular signals into diverse cellular responses[37]. Abnormalities in MAPK pathways are associated with many diseases, including inflammatory disease, immune diseases, degenerative diseases, diabetes, and tumors[38]. There are three major MAPK pathways: extracellular signal-regulated kinases 1/2 (ERK1/2), c-Jun amino (N)-terminal kinase (JNK), and p38. Previous research has shown that these three pathways synergistically regulate osteoclasts. ERK signaling seems to be more closely associated with osteoclast precursor cells. In response to

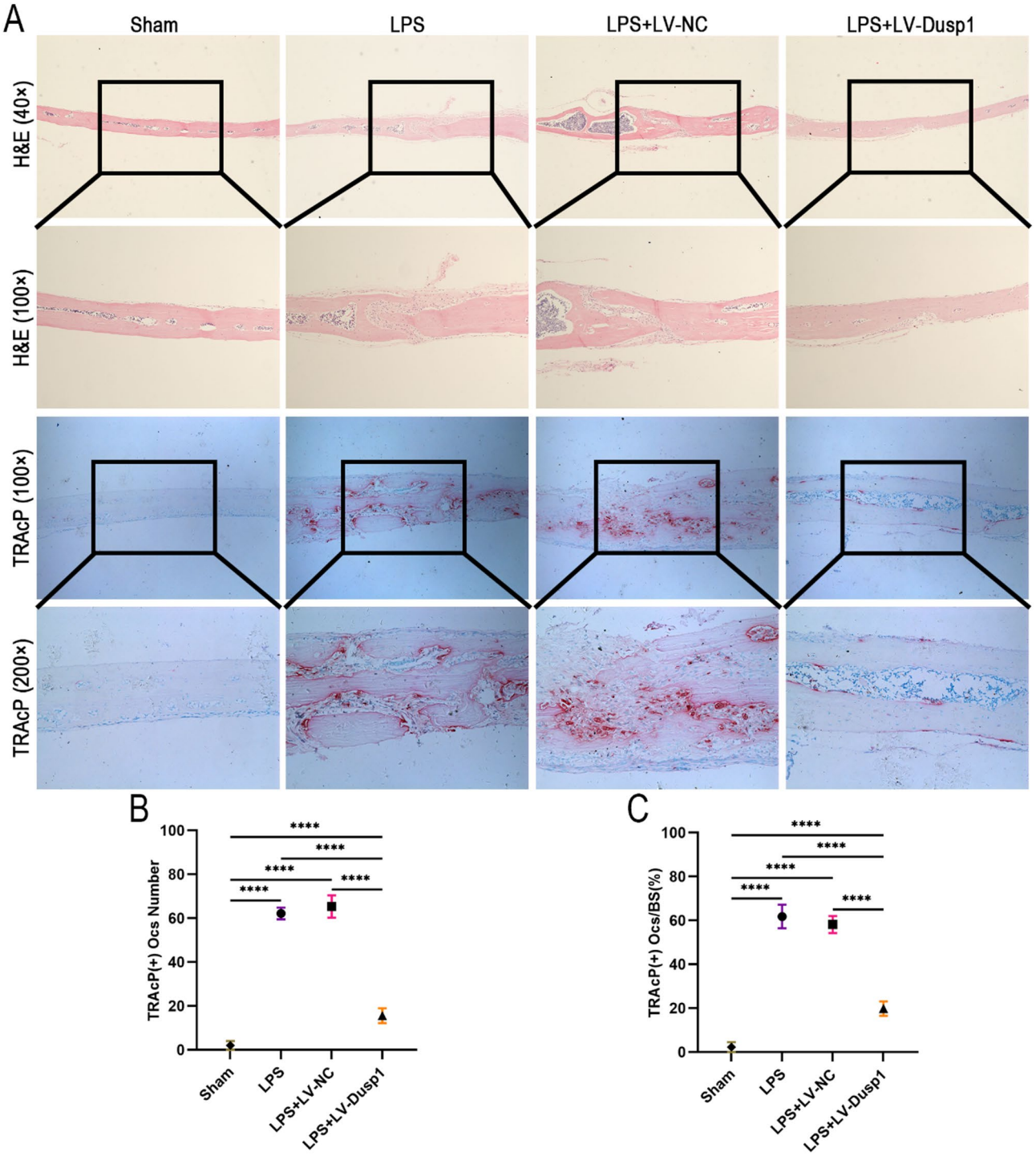

Fig. 7. Dusp1 reduced osteoclast number and activity in vivo and prevented LPS-induced mice skull osteolysis. (**A**) H&E and TRAcP staining images of mice skulls. (**B**, **C**) Quantification of the number of TRAcP-positive osteoclasts and the area of TRAcP-positive osteoclasts per bone surface (Oc.S/BS). Data are presented as mean ± SD (n = 5). ****$p < 0.0001$.

M-CSF stimulation, ERK signaling supports the survival and differentiation of osteoclast precursor cells[39]. JNK signaling plays an anti-apoptotic role in RANKL-induced osteoclast maturation to stabilize osteoclast differentiation[40]. Blocking JNK signaling specifically, while leaving p38 and ERK unaffected, has been shown to promote osteoclast apoptosis[41]. In addition, ERK and JNK signal cooperatively control transcription factors such as c-FOS. Phosphorylated ERK activates c-FOS by phosphorylating specific serine residues (362 and 374), while phosphorylated JNK activates c-Jun, which then forms the AP-1 complex with c-FOS[42]. In contrast, P38 signaling is more involved in the metabolism of mature osteoclasts. By triggering the transcription factor NFATc1,

P38 signaling induces the expression of downstream osteoclast-specific genes. The sustained activity of these genes maintains the bone resorption function of osteoclasts[43]. Our study found that the total protein content of ERK, JNK and P38 in osteoclasts was not affected by RANKL stimulation. But their activated phosphorylated protein increased substantially after 5 to 20 min of RANKL stimulation. However, Dusp1 overexpression via lentivirus transfection treatment antagonized the function of RANKL. This phenomenon reveals that Dusp1 comprehensively inhibits the MAPK signaling pathway through the ERK, JNK and P38 pathways. Our findings may explain how Dusp1 downregulates downstream key transcription factors c-FOS and NFATc1, thereby suppressing osteoclast-specific genes. This molecular mechanism may contribute to Dusp1's role in osteolytic disease pathogenesis. To investigate the therapeutic potential of Dusp1 in osteolytic diseases, we performed in vivo validation using animal models.

As an endotoxin released by gram-negative bacteria, LPS can be absorbed by the body through the gastrointestinal tract[44]. LPS induces inflammation by stimulating immune cells to secret proinflammatory cytokines including interleukin and tumor necrosis factor[45]. Inflammation mediated by LPS is associated with many diseases, including sepsis, neurodegenerative diseases, metabolic diseases, and cardiovascular disease[46]. Patients with inflammatory related diseases usually have low bone mineral density, and more and more studies have shown that inflammatory factors can cause osteolysis or bone loss[47,48]. LPS suppresses osteoblast differentiation and bone formation by reducing the synthesis of various osteoblast transcription factors[49]. Also, LPS can recruit osteoclast precursor cells, stimulate the production of M-CSF and RANKL[50]. In addition, LPS increases osteoclast differentiation and activity by phosphorylating MAPK pathway proteins, thereby promoting bone resorption[51]. Animal experiments found that LPS treatment promoted osteoclast activity, destroyed bone trabecula, and caused bone mass loss[52]. Currently, rodent models treated with LPS are often used to study inflammatory osteolysis or bone loss. Hence, we used LPS to induce skull osteolysis in mice and treated them with Dusp1 overexpression lentivirus. Lentiviral transfection may lead to undesired Dusp1 overexpression in other cell types. For instance, Dusp1 overexpression in immune cells could potentially suppress immune responses and increase susceptibility to acute infections. To minimize systemic effects of lentiviral delivery in our murine model, we employed localized injection protocols. The results showed that LPS caused severe damage to mice skulls and many mature osteoclasts infiltrated into the lesion area. As a result of Dusp1 overexpression lentivirus treatment, there was less bone resorption extent and fewer TRAcP-positive osteoclasts. Our study indicated that Dusp1 prevents inflammatory osteolysis through targeting osteoclasts.

Our study has established that Dusp1 suppresses osteoclasts by downregulating the MAPK/c-FOS/NFATc1 signaling pathway (Fig. 8). Nevertheless, potential involvement of Dusp1 in osteolytic diseases via other mechanisms warrants further investigation. Dusp1 is involved in glucose metabolism and its expression is modulated by blood glucose levels[53]. Interestingly, glucose sensing and O-GlcNAcylation processes can potentiate osteoclast activity[54]. These findings suggest that Dusp1 may intersect with certain metabolic signals or nutrient sensing pathways during osteoclastogenesis. Furthermore, due to the importance of osteoblasts in maintaining bone homeostasis, it is necessary to explore the role of Dusp1 on osteoblasts.

In summary, our study demonstrated that Dusp1 reduces osteoclast number and activity and provides protection against LPS-induced osteolysis. Inhibiting the MAPK/c-FOS/NFATc1 signaling pathway may be one of its molecular mechanisms. Therefore, upregulating Dusp1 has the potential to be a novel therapeutic approach for treating osteolytic diseases.

Materials and methods

Materials and reagents

Alpha modification of minimal essential medium (α-MEM) was purchased from Thermo Fisher Scientific (Massachusetts, USA). Fetal bovine serum (FBS) was purchased from Avantor (Pennsylvania, USA). Recombinant mice M-CSF and RANKL were obtained from LifeTein (New Jersey, USA). Phosphate buffered solution (PBS), penicillin/streptomycin (P/S), polybrene, puromycin, Immunostaining Permeabilization Buffer with Triton X-100, and 2-(4-Amidinophenyl)-6-indolecarbamidine dihydrochloride (DAPI) staining solution were purchased from Beyotime (Shanghai, China). Tetramethyl rhodamine isothio-cyanate (TRITC) Phalloidin, 4% paraformaldehyde (PFA), bovine serum albumin (BSA) blocking buffer and tartrate-resistant acid phosphatase (TRAcP) staining kit were purchased from Solarbio (Beijing, China). Lipopolysaccharide (LPS) was purchased from Sigma-Aldrich (Missouri, USA). Antibodies against Dusp1, phospho-JNK, JNK, phospho-ERK, ERK, phospho-P38, P38, NFATc1, c-Fos, CTSK, GAPDH, α-Tubulin, and β-actin were purchased from Cell Signaling Technology (Massachusetts, USA). Secondary antibodies were purchased from Thermo Fisher Scientific (Massachusetts, USA).

Cell extraction and osteoclast differentiation in vitro

Six-week-old C57/BL6J mice were euthanized, then the femur and tibia marrow cavities were rinsed under sterile conditions immediately. The rinse solution was filtered through a 0.45um filter and centrifuged at 1000 rpm for 5 min. Extracted cells were resuspended in α-MEM with 1% P/S, 10% FBS, and 30 ng/ml M-CSF. Then the cells were transferred to culture flasks and placed in an incubator with 5% carbon dioxide at 37℃. The medium was replaced after 2 days, and bone marrow-derived macrophages (BMMs) for subsequent experiments were obtained after 4 days. The BMMs were plated and cultured in complete medium supplemented with M-CSF. After 12 h, the medium was replaced with osteoclastogenic medium (complete medium with 30 ng/ml M-CSF and 50 ng/mL RANKL) to induce osteoclast differentiation. Mature osteoclasts typically developed after 5–7 days.

Lentivirus packaging and tittering

A recombinant vector was constructed by connecting a lentiviral vector with either a negative control (NC) or Dusp1 deoxyribonucleic acid (DNA). The pCMV-dR8.9 (Addgene, USA) and pCMV-VSV-G (Addgene,

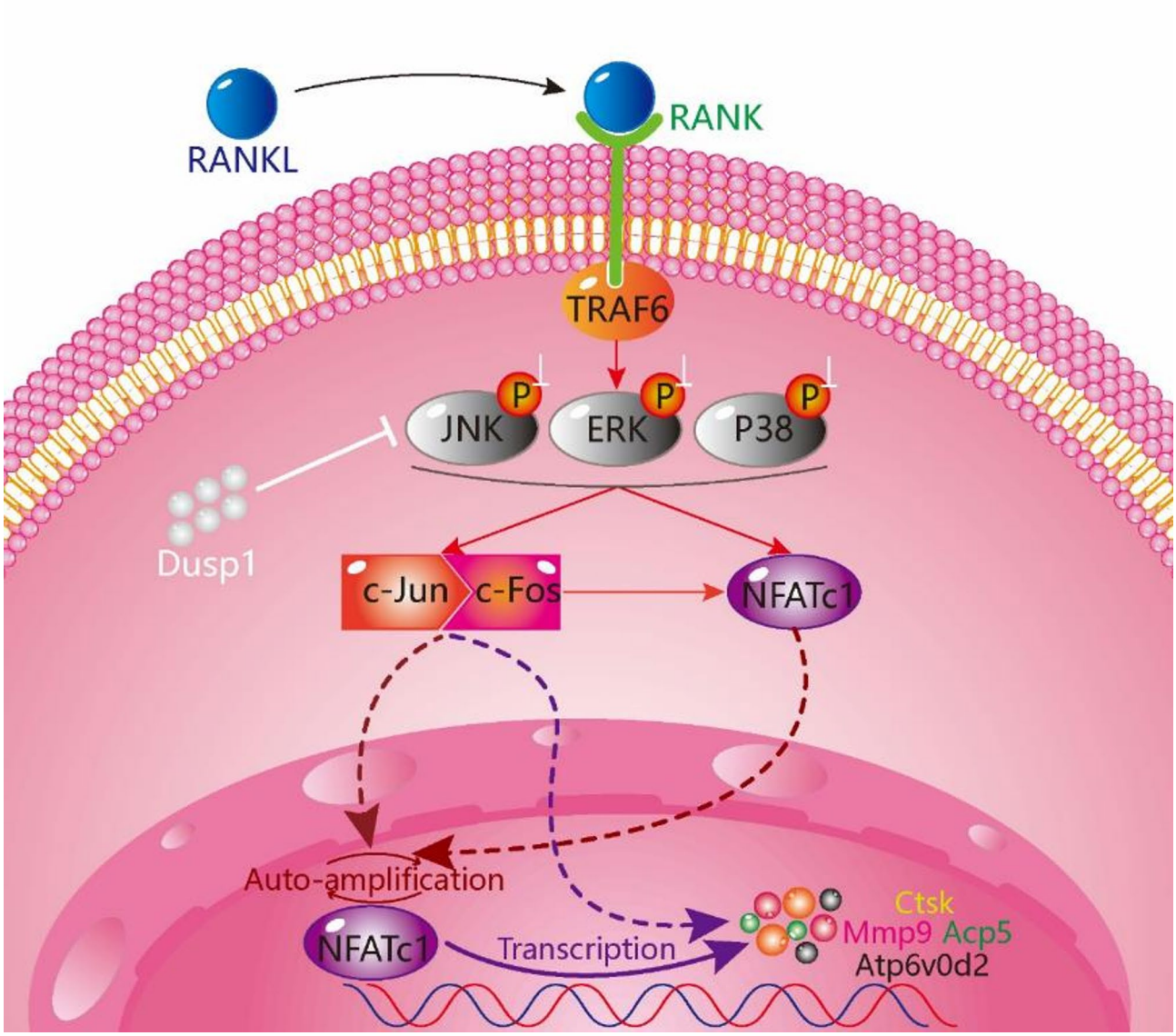

Fig. 8. Schematic diagram of Dusp1 suppresses osteoclast differentiation. Dusp1 inactivates MAPK signaling, down-regulates c-FOS and NFATc1, and inhibits osteoclast-specific genes, thereby suppressing osteoclast activity.

USA) packaging plasmids were used for lentiviral packaging. The transfection complex was co-transfected into HEK293T cells. After 48–72 h, the viral supernatants were collected, filtered through 0.22um filters, and concentrated using an ultracentrifugation device (Beckman SW28, BECKMAN COULTER, USA). The virus titer was determined by quantitative real-time polymerase chain reaction (qPCR).

Target cell transduction

Primary BMMs were seeded in 6-well (1×10^5 cells/well) or 96-well (6×10^3 cells/well) plates. The cells were cultured with complete medium containing M-CSF at a density of 30% to 50%. After 12 h (marked as D0), osteoclastogenic medium (complete medium with 30 ng/ml M-CSF and 50 ng/ml RANKL) was replaced to induce osteoclast differentiation. At the same time, the BMMs were transduced with lentivirus at a multiplicity of infection (MOI) of 100 using polybrene. After 24 h of transfection (D1), the medium containing lentivirus was removed. Osteoclastogenic medium containing puromycin was replaced every 48 h to screen for stable transfected cells. After 72 h of transfection (D3), the transfection efficiency was confirmed through imaging of the green fluorescence protein.

F-actin ring staining

Primary BMMs were seeded on 96-well cell culture plates. The cells were then transfected with NC or Dusp1 overexpression lentivirus and cultured in osteoclastogenic medium for 6 days. After being fixed by 4% PFA for 30 min, the cells were treated with 0.1% Triton X-100 for 10 min and blocked by 3% BSA for 1 h. Subsequently,

Genes	Forward (5′–3′)	Reverse (5′–3′)
Dusp1	TTGTCGCTCCTTCTTCGCTT	TCAGCGTTGGGCACGATATG
Ctsk	TTCCAGTTTTACAGCAGAGGTGT	AGTGCTTGCTTCCCTTCTGG
Fos	CCAGTCAAGAGCATCAGCAA	AAGTAGTGCAGCCCGGAGTA
Nfatc1	TGTGCAAGCCAAATTCCCT	ACAGAGTTACCATTGGCAGG
Mmp9	CAAAGACCTGAAAACCTCCAAC	GACTGCTTCTCTCCCATCATC
Acp5	ACACAGTGATGCTGTGTGGCAACTC	CCAGAGGCTTCCACATATATGATGG
Atp6v0d2	GTGAGACCTTGGAAGACCTGAA	GAGAAATGTGCTCAGGGGCT
β-actin	TGTCCACCTTCCAGCAGATGT	GCTCAGTAACAGTCCGCCTAGA

Table 1. Primer sequences for qPCR.

the cells were stained by TRITC Phalloidin for 2 h. Finally, DAPI was used to counterstain the cells for 5 min. The EVOS FL Auto2 imaging system was used to take photos, and ImageJ v1.8.0 was used to analyze images. The number and area of F-actin ring were calculated.

TRAcP staining

Primary BMMs were seeded on 96-well cell culture plates. Osteoclastogenic medium was used to induce osteoclast differentiation and replaced every 2 days. Six days post-transfection with either NC or Dusp1 overexpression lentivirus, the cells were fixed with 4% PFA for 30 min. TRAcP staining was then performed according to the instruction. EVOS FL Auto2 imaging system (Thermo Fisher Scientific, USA) was used to capture images. Images were analyzed by ImageJ v1.8.0. Mature osteoclasts identified by TRAcP positivity and having more than three nuclei were quantified.

Bone resorption assay

Sterile bovine bone slices were placed into 96-well cell culture plates, followed by the seeding of primary BMMs. The BMMs were transfected with NC or Dusp1 overexpression lentivirus and cultured with osteoclastogenic medium for about six days. At that time, mature osteoclasts could be seen through the observation wells. After another 2 days, the cells on the surface of the bone slices were removed by ultrasound. The bone resorption area was scanned with an electron microscope (Regulus 8100, HITACHI, Japan) and quantified using ImageJ v1.8.0.

RNA extraction and qPCR

Primary BMMs were seeded on 6-well plates. Five days after the BMMs were transfected with NC or Dusp1 overexpression lentivirus and cultured with osteoclastogenic medium, Trizol reagent was used to extract total ribonucleic acid (RNA). Then, cDNA was synthesized using the cDNA Synthesis Kit (Thermo Fisher Scientific, USA). The qPCR was performed using the StepOne System (Thermo Fisher Scientific, USA). The reaction procedure consisted of an initial denaturation at 95℃ for 10 min, followed by 40 cycles of 95℃ for 10 s and 60℃ for 30 s. A melt curve analysis was then conducted, starting at 95℃ for 15 s, cooling to 60℃ for 1 min, and finishing with a final heating at 95℃ for 15 s. The relative expression levels of target genes were calculated using the $2^{-\Delta\Delta CT}$ method. The primer sequences used for the experiment are shown in Table 1.

Protein extraction and western blot analysis

Primary BMMs were seeded on 6-well plates. After 12 h (D0), the BMMs were transfected with NC or Dusp1 overexpression lentivirus and cultured in osteoclastogenic medium. Total protein was extracted to assess Dusp1 expression on D5. The expressions of NFATc1, c-Fos, and CTSK were analyzed on D0, D1, D3, and D5. A different processing method was used to determine if Dusp1 mediates the RANKL-induced MAPK signaling pathway in osteoclasts. The BMMs transfected with NC or Dusp1 overexpression lentivirus were cultured with complete medium containing M-CSF until they reached nearly 100% confluence. Afterwards, they were serum-starved for 4 h before being stimulated with RANKL for 0, 5, 10, 20, 30, and 60 min. Protein extraction was performed immediately following stimulation.

The extraction of total proteins was carried out according to the instruction of the Column Tissue & Cell Protein Extraction Kit (Epizyme, China). Protein electrophoresis was performed using gels prepared by the Easy PAGE® Gel Fast Preparation Kit (10%) (SEVEN BIOTECH, China) at 120 V for 60 min. Then proteins were transferred to polyvinylidene difluoride (PVDF) membranes (Merck, Germany). Afterwards, the membranes were blocked in 5% skim milk for 1.5 h, followed by incubation with specific primary antibodies at 4℃ for 12 h and fluorescence-labeled secondary antibodies for 1 h. An Odyssey (LI-COR Biosciences, USA) near-infrared fluorescence imaging scanner was used to scan. ImageJ v1.8.0 was used to analyze the grayscale values of the protein bands. The quantification was performed under blind conditions.

LPS-induced skull osteolysis animal model

This study followed the guidelines of the Animal Ethics Committee of Guangxi Medical University. Twenty 6-week-old mice purchased from the Animal Experiment Center of Guangxi Medical University were randomly divided into four groups (5 mice per group): Sham group (PBS, control), LPS group (LPS, 5 mg/kg body weight), LPS + LV-NC group (LPS, 5 mg/kg with NC lentivirus, 1×10^9 transduction units), and LPS + LV-Dusp1 group (LPS, 5 mg/kg with Dusp1 overexpression lentivirus, 1×10^9 transduction units). Isoflurane was used to

anesthetize the mice. The volume and concentration of the injected lentivirus were based on previous studies[55,56]. Mice in the LPS + LV-NC and LPS + LV-Dusp1 groups received subcutaneous injections of 20 µl lentivirus (5×10^8 TU/ml) one day before the first LPS treatment. Subsequent subcutaneous injections of PBS or LPS were administered every two days at the sagittal midline suture of the skull. After 14 days, the mice were euthanized by inhalation of 50% carbon dioxide, and their skulls were collected for further analysis. All experimental protocols were approved by the Animal Ethics Committee of Guangxi Medical University (No.202212012). All methods were carried out in accordance with relevant guidelines and regulations. All methods are reported in accordance with ARRIVE guidelines.

Micro-CT scanning and analysis

The mice skulls were separated and fixed with 4% paraformaldehyde. Micro-CT scanning was performed using a Skyscan 1275 X-Ray Microtomograph (Bruker, USA). The voltage was 46 kV, the current was 75 µA, and the resolution was 10 µm. The 3D images were reconstructed using Skyscan CTAn software. The osteolysis areas adjacent to the sagittal midline suture of the skulls were analyzed. The bone volume/tissue volume ratio (BV/TV), number of porosity, and percentage of porosity were calculated.

Histological analysis

Histological analysis was performed following micro-CT scanning. The skull samples were decalcified in 10% ethylene diamine tetraacetic acid (EDTA) at 4℃ for 2 weeks. After being embedded with paraffin, the samples were cut into 5 µm sections for hematoxylin and eosin (H&E) and TRAcP staining. The number of TRAcP-positive osteoclasts and the area of TRAcP-positive osteoclasts per bone surface (Oc.S/BS) were measured using ImageJ v1.8.0.

Statistical analysis

Data were presented as mean ± standard deviation (SD) and analyzed using ANOVA or Student's t-test by GraphPad Prism 9.1. $P < 0.05$ was considered statistically significant.

Data availability statement

All data generated or analysed during this study are included in this published article and its supplementary information files.

Received: 16 March 2025; Accepted: 30 May 2025
Published online: 01 July 2025

References

1. Datta, H. K., Ng, W. F., Walker, J. A., Tuck, S. P. & Varanasi, S. S. The cell biology of bone metabolism. *J. Clin Pathol.* **61**, 577–587 (2008).
2. Győri, D. S. & Mócsai, A. Osteoclast signal transduction during bone metastasis formation. *Front. Cell Dev Biol.* **8**, 507 (2020).
3. Muruganandan, S., Dranse, H. J., Rourke, J. L., McMullen, N. M. & Sinal, C. J. Chemerin neutralization blocks hematopoietic stem cell osteoclastogenesis. *Stem Cells.* **31**, 2172–2182 (2013).
4. Takegahara, N., Kim, H. & Choi, Y. Unraveling the intricacies of osteoclast differentiation and maturation: insight into novel therapeutic strategies for bone-destructive diseases. *Exp. Mol Med.* **56**, 264–272 (2024).
5. Inoue, K. et al. Bone marrow Adipoq-lineage progenitors are a major cellular source of M-CSF that dominates bone marrow macrophage development, osteoclastogenesis, and bone mass. *Elife* **12**, e82118 (2023).
6. Hu, Y. et al. RANKL from bone marrow adipose lineage cells promotes osteoclast formation and bone loss. *EMBO. Rep.* **22**, e52481 (2021).
7. Liu, T. et al. Tereticornate A suppresses RANKL-induced osteoclastogenesis via the downregulation of c-Src and TRAF6 and the inhibition of RANK signaling pathways. *Biomed. Pharmacother.* **151**, 113140 (2022).
8. Omata, Y., Tachibana, H., Aizaki, Y., Mimura, T. & Sato, K. Essentiality of Nfatc1 short isoform in osteoclast differentiation and its self-regulation. *Sci. Rep.* **13**, 18797 (2023).
9. Gregson, C. L. et al. UK clinical guideline for the prevention and treatment of osteoporosis. *Arch. Osteoporos.* **17**, 58 (2022).
10. Deng, Y. L. et al. Predictors for self-discontinuation of anti-osteoporosis medication: A hospital-based real-world study. *PLoS ONE* **17**, e0275020 (2022).
11. Ayers, C. et al. Effectiveness and safety of treatments to Prevent fractures in people with low bone mass or primary osteoporosis: A living systematic review and network meta-analysis for the American College of Physicians. *Ann. Intern Med.* **176**, 182–195 (2023).
12. Pan, M. et al. Drugs for the treatment of postmenopausal symptoms: Hormonal and non-hormonal therapy. *Life. Sci.* **312**, 121255 (2023).
13. Zheng, J. et al. Lowering of circulating sclerostin may increase risk of atherosclerosis and its risk factors: Evidence from a genome-wide association meta-analysis followed by mendelian randomization. *Arthritis. Rheumatol.* **75**, 1781–1792 (2023).
14. Guañabens, N. et al. The next step after anti-osteoporotic drug discontinuation: An up-to-date review of sequential treatment. *Endocrine* **64**, 441–455 (2019).
15. Foessl, I., Dimai, H. P. & Obermayer-Pietsch, B. Long-term and sequential treatment for osteoporosis. *Nat. Rev Endocrinol.* **19**, 520–533 (2023).
16. Cimas, F. J., Callejas-Valera, J. C. & Sanchez-Prieto, R. MKP1: Jekyll and Hyde for E1A. *Aging (Albany NY).* **8**, 214–215 (2016).
17. Martínez-Martínez, D. et al. Downregulation of snail by DUSP1 impairs cell migration and invasion through the inactivation of JNK and ERK and is useful as a predictive factor in the prognosis of prostate cancer. *Cancers (Basel).* **13,** 1158 (2021).
18. Lee, K., Seo, I., Choi, M. H. & Jeong, D. Roles of mitogen-activated protein kinases in osteoclast biology. *Int J. Mol Sci.* **19**, 3004 (2018).
19. Ambrosi, T. H. et al. Aged skeletal stem cells generate an inflammatory degenerative niche. *Nature*. **597,** 256–262 (2021).
20. Huber, R. et al. Identification of intra-group, inter-individual, and gene-specific variances in mRNA expression profiles in the rheumatoid arthritis synovial membrane. *Arthritis. Res Ther.* **10**, R98 (2008).
21. Sartori, R., Li, F. & Kirkwood, K. L. MAP kinase phosphatase-1 protects against inflammatory bone loss. *J. Dent Res.* **88**, 1125–1130 (2009).
22. Kim, J. M., Lin, C., Stavre, Z., Greenblatt, M. B. & Shim, J. H. Osteoblast-osteoclast communication and bone homeostasis. *Cells* **10**, 2073 (2020).

23. Reid, I. R. & Billington, E. O. Drug therapy for osteoporosis in older adults. *Lancet* **399**, 1080–1092 (2022).
24. Khadir, A. et al. MAP kinase phosphatase DUSP1 is overexpressed in obese humans and modulated by physical exercise. *Am J. Physiol Endocrinol Metab.* **308**, E71-83 (2015).
25. Strebinger, D. et al. Cell type-specific delivery by modular envelope design. *Nat. Commun.* **14**, 5141 (2023).
26. An, D. S. et al. Optimization and functional effects of stable short hairpin RNA expression in primary human lymphocytes via lentiviral vectors. *Mol. Ther.* **14**, 494–504 (2006).
27. Portes, M. et al. Nanoscale architecture and coordination of actin cores within the sealing zone of human osteoclasts. *Elife* **11**, e75610 (2022).
28. Shen, S. et al. Leucine repeat rich kinase 1 controls osteoclast activity by managing lysosomal trafficking and secretion. *Biology (Basel)*. **12,** 511 (2023).
29. Ke, D., Yu, Y., Li, C., Han, J. & Xu, J. Phosphorylation of BCL2 at the Ser70 site mediates RANKL-induced osteoclast precursor autophagy and osteoclastogenesis. *Mol. Med.* **28**, 22 (2022).
30. Wang, Y. et al. MCU inhibitor ruthenium red alleviates the osteoclastogenesis and ovariectomized osteoporosis via suppressing RANKL-induced ROS production and NFATc1 activation through P38 MAPK signaling pathway. *Oxid. Med Cell Longev.* **2022**, 7727006 (2022).
31. Asagiri, M. et al. Autoamplification of NFATc1 expression determines its essential role in bone homeostasis. *J. Exp Med.* **202**, 1261–1269 (2005).
32. He, J. et al. Inhibitory effects of Rhaponticin on osteoclast formation and resorption by targeting RANKL-induced NFATc1 and ROS activity. *Front. Pharmacol.* **12**, 645140 (2021).
33. Wu, H., Xu, G. & Li, Y. P. Atp6v0d2 is an essential component of the osteoclast-specific proton pump that mediates extracellular acidification in bone resorption. *J. Bone Miner Res.* **24**, 871–885 (2009).
34. Miyamoto, T. Regulators of osteoclast differentiation and cell–cell fusion. *Keio. J. Med.* **60**, 101–105 (2011).
35. Matsuo, K. et al. Fosl1 is a transcriptional target of c-Fos during osteoclast differentiation. *Nat. Genet.* **24**, 184–187 (2000).
36. Pang, M. et al. AP-1 and Mitf interact with NFATc1 to stimulate cathepsin K promoter activity in osteoclast precursors. *J. Cell Biochem.* **120**, 12382–12392 (2019).
37. Gałgańska, H., Jarmuszkiewicz, W., Gałgański, Ł. Carbon dioxide and MAPK signalling: towards therapy for inflammation. *Cell Commun Signal.* **21,** 280 (2023).
38. Loukas, A. T. et al. Natural compounds for bone remodeling: a computational and experimental approach targeting bone metabolism-related proteins. *Int J. Mol Sci.* **25**, 5047 (2024).
39. Ross, F. P. M-CSF, c-Fms, and signaling in osteoclasts and their precursors. *Ann. N Y. Acad Sci.* **1068**, 110–116 (2006).
40. Ikeda, F. et al. JNK/c-Jun signaling mediates an anti-apoptotic effect of RANKL in osteoclasts. *J. Bone Miner Res.* **23**, 907–914 (2008).
41. Mozar, A. et al. High extracellular inorganic phosphate concentration inhibits RANK-RANKL signaling in osteoclast-like cells. *J. Cell Physiol.* **215**, 47–54 (2008).
42. Wagner, E. F., Matsuo, K. Signalling in osteoclasts and the role of Fos/AP1 proteins. *Ann. Rheum Dis*. **62 Suppl 2,** ii83–85 (2003).
43. Matsumoto, M. et al. Essential role of p38 mitogen-activated protein kinase in cathepsin K gene expression during osteoclastogenesis through association of NFATc1 and PU.1. *J. Biol. Chem*. **279,** 45969–45979 (2004).
44. Ghosh, S. S., Wang, J., Yannie, P. J. Ghosh, S. Intestinal barrier dysfunction, LPS translocation, and disease development. *J. Endocr. Soc*. **4,** bvz039 (2020).
45. Park, S. et al. SIRT1 alleviates LPS-induced IL-1β production by suppressing NLRP3 inflammasome activation and ROS production in trophoblasts. *Cells* **9**, 728 (2020).
46. Brown, G. C. & Heneka, M. T. The endotoxin hypothesis of Alzheimer's disease. *Mol. Neurodegener.* **19**, 30 (2024).
47. Brandt, I. A. G., Starup-Linde, J., Andersen, S. S. & Viggers, R. Diagnosing osteoporosis in diabetes-A systematic review on BMD and fractures. *Curr. Osteoporos Rep.* **22**, 223–244 (2024).
48. Dai, Z. et al. Two-sample Mendelian randomization analysis evaluates causal associations between inflammatory bowel disease and osteoporosis. *Front. Public Health.* **11**, 1151837 (2023).
49. Bandow, K. et al. Molecular mechanisms of the inhibitory effect of lipopolysaccharide (LPS) on osteoblast differentiation. *Biochem. Biophys Res Commun.* **402**, 755–761 (2010).
50. Kikuchi, T. et al. Gene expression of osteoclast differentiation factor is induced by lipopolysaccharide in mouse osteoblasts via Toll-like receptors. *J. Immunol.* **166**, 3574–3579 (2001).
51. Bi, Y. et al. Adherent endotoxin on orthopedic wear particles stimulates cytokine production and osteoclast differentiation. *J. Bone Miner Res.* **16**, 2082–2091 (2001).
52. Bott, KN. et al. Lipopolysaccharide-induced bone loss in rodent models: a systematic review and meta-analysis. *J. Bone Miner Res.* **38,** 198–213 (2023).
53. Begum, N. & Ragolia, L. High glucose and insulin inhibit VSMC MKP-1 expression by blocking iNOS via p38 MAPK activation. *Am J. Physiol Cell Physiol.* **278**, C81-91 (2000).
54. Taira TM. et al. HBP/O-GlcNAcylation metabolic axis regulates bone resorption outcome. *J. Dent Res*. **102,** 440–449 (2023).
55. Zeng, H. et al. Lentivirus-mediated downregulation of α-synuclein reduces neuroinflammation and promotes functional recovery in rats with spinal cord injury. *J. Neuroinflammation.* **16**, 283 (2019).
56. Skukan, L. et al. Lentivirus- or AAV-mediated gene therapy interventions in ischemic stroke: A systematic review of preclinical in vivo studies. *J. Cereb Blood Flow Metab.* **42**, 219–236 (2022).

Author contributions

S. Z. and G. Z. designed the study. B. L., M. L., B. W., Y. F., Y. T. , D.X., and S. C. participated in the experiment and data analysis. B.L. prepared the figures and drafted the original manuscript. S. Z. and G.Z. revised the manuscript and supervised the project. All authors reviewed and approved the final manuscript.

Funding

The research was supported by the Joint Project on Regional High-Incidence Disease Research of Guangxi Natural Science Foundation under Grant No. 2024GXNSFDA010035 and the Guangxi Medical High-level Key Talents Training "139" Program (No. (2020)15).

Declarations

Competing interests

The authors declare no competing interests.

Ethics approval and consent to participate

The Animal Ethics Committee of Guangxi Medical University approved the study (No. 202212012).

Patients consent for publication

This study does not involve human subjects or human tissue.

Additional information

Supplementary Information The online version contains supplementary material available at https://doi.org/10.1038/s41598-025-05142-6.

Correspondence and requests for materials should be addressed to G.Z. or S.Z.

Reprints and permissions information is available at www.nature.com/reprints.

Publisher's note Springer Nature remains neutral with regard to jurisdictional claims in published maps and institutional affiliations.